RSC Advances

PAPER

View Article Online
View Journal | View Issue

Cite this: *RSC Adv.*, 2020, **10**, 2241

Collagen–curcumin nanocomposites showing an enhanced neuroprotective effect against short term focal cerebral ischemia†

Pankaj Rathore,[a] Indu Arora,[b] Shweta Rastogi,[c] Mohd. Akhtar,[d] Shruti Singh[e] and Mohammed Samim *[a]

Received 17th October 2019
Accepted 5th January 2020

DOI: 10.1039/c9ra08508d

rsc.li/rsc-advances

The effectiveness of curcumin in treating cerebral ischemia has been reported in recent studies. However, its mode of action is still not defined. The objective of the present study is to formulate collagen–curcumin nanocomposites which will work effectively against cerebral ischemia/reperfusion injury. Ischemic injury is followed by inflammatory damage and oxidative stress, which together contribute a lot in the pathogenesis of cerebral ischemia and may be considered a good target for treatment. The present study focused on examining the effectiveness of collagen–curcumin nanocomposites stabilized by increasing the degree of crosslinking in reducing oxidative stress associated with brain injury resulting from cerebral ischemia. The collagen nanoparticles were prepared by conjugating collagen on the surface of Tween©80 micelles, and further stabilizing them using crosslinkers. The effectiveness of the prepared nanocomposite was validated by performing infarct analysis followed by biochemical, behavioral, histopathological and immunohistochemical studies. The outcomes of this study are promising for the use of collagen–curcumin nanocomposites in showing neuroprotective potential in treating ischemic injury.

1. Introduction

In the last few decades cerebral ischemia related brain injuries have become a central cause of human deaths and disabilities across the world.[1] Ischemic stroke occurs when blood supply to the brain is reduced due to blockage in the arteries supplying blood and oxygen to the brain. This restricted oxygen supply, also known as cerebral hypoxia, results in the formation of a region of necrotic tissue, termed cerebral infarction. Recent studies have proved that cerebral ischemia/reperfusion injury-induced neuronal brain damage is a result of a series of pathological processes like oxidative stress, inflammatory reactions, disruption of the blood–brain barrier (BBB) and neuronal apoptosis.[2] MCAO is a well-characterized and classical model that has proved to be invaluably useful for studying the pathophysiology of focal cerebral ischemia.[3,4] Several mechanisms including *N*-methyl-D-aspartate (NMDA) receptor activation leading to excitotoxicity, excessive nitric oxide (NO) generation and free radical-mediated oxidative stress are involved in the cascade of neuronal deaths.[5,6] In addition to that, the generation of excess free radicals and impairment of antioxidant defense mechanism causes more vulnerability and damage to the brain.[7]

The blood–brain barrier poses the biggest challenge in treating neurodegenerative diseases,[8] due to its limited permeability and restrictions to the entry of the drug into the brain. This not only results in reduced drug efficacy but also makes it necessary to administer a high dose of the drug to achieve the desired effect. However, high doses inadvertently lead to harmful side effects. In the last few decades therapeutic potential of curcumin, a well-known traditional spice, has been explored for treating central nervous system (CNS) diseases and is found to be extremely effective, possibly due to its anti-inflammatory and anti-oxidant properties.[9] Neuroprotective potential of curcumin is not only because of its antioxidant properties but also due to it being able to cross the blood–brain barrier though in trace amounts.[10] Several studies have shown administering curcumin after ischemia shows protective effects like diminished lipid peroxidation, mitochondrial dysfunction, glial activation, improved neurological scores, and locomotor activities.[11] Despite having so many traits the neuroprotective efficacy of curcumin has been limited by poor aqueous solubility, rapid metabolism and fast elimination from circulation.

[a]Department of Chemistry, School of Chemical & Life Sciences, Jamia Hamdard, New Delhi-62, India. E-mail: shamim_chem@yahoo.co.in
[b]Department of Biomedical Sciences, Shaheed Rajguru College, Delhi University, New Delhi, India
[c]Department of Chemistry, Hansraj College, Delhi University, Delhi, India
[d]Department of Pharmacology, School of Pharmaceutical Education & Research, Jamia Hamdard, New Delhi-62, India
[e]Department of Botany, School of Chemical & Life Sciences, Jamia Hamdard, New Delhi-62, India

† Electronic supplementary information (ESI) available. See DOI: 10.1039/c9ra08508d

Here, polymeric micelle based nanoparticles having distinct advantages like higher drug loading capacity, increased solubility of hydrophobic drugs and sustained release of drugs, could prove to be boon in overcoming the hurdles involved in brain drug delivery. Thus, providing a viable option as a nanocarrier for transporting active molecules across BBB. The main objective of the present study is to design and prepare curcumin loaded collagen conjugated Tween©80 nanoparticles for brain drug delivery using a simple but highly efficient preparation methodology. The efficiency of the formulation was further proved by studying the effects of using collagen–curcumin nanocomposite in comparison with free curcumin on various *in vivo* investigations. Biopolymer collagen was chosen as it is cytocompatible, biodegradable and easily available,[12] but it lacks the mechanical properties and aqueous stability required for medical applications so the cross-linking approach was followed to overcome these limitations. Collagen nanoparticles have been stabilized by using 1-ethyl-3-(3-dimethyl aminopropyl)carbodiimide-hydrochloride (EDC·HCl) and malondialdehyde (MDA) as crosslinkers for attaining a slow and sustained drug release. The collagen nanoparticles are brain targeted using Tween©80, that helps in the passage of drug across BBB by mimicking through low-density lipoproteins (LDL) present on the surface of the brain.[13] Tween©80, a polysorbate, is an amphipathic non-ionic surfactant made of fatty acid esters of polyethylene sorbitan. Micelles are formed by spherical aggregation of polysorbate in which the hydrocarbon chain makes the hydrophobic part that points towards the center and the hydrophilic part consists of ethylene oxide subunits pointing towards outside, in contact with the surrounding solution. Curcumin being hydrophobic goes into the core of micelle forming van der Waals bond with hydrophobic polymer core thus stabilizing micelle, similarly, hydrogen bonding of hydrophilic corona with surroundings also stabilizes the micelle.

2. Experimental section

2.1 Chemicals & reagents

Chemicals procured from SRL limited [glutathione reductase (GR), oxidized glutathione (GSSG), 1,2-dithio-bis-nitrobenzoic acid (DTNB), reduced nicotinamide adenine dinucleotide phosphate (NADPH), 1-chloro-2,4-dinitrobenzene (CDNB), sodium hydroxide (NaOH), trichloroacetic acid (TCA), copper sulfate ($CuSO_4$), ethylenediaminetetraacetic acid (EDTA), disodium orthophosphate (Na_2HPO_4), sodium dihydrogen phosphate (NaH_2PO_4), sodium potassium tartrate, sodium carbonate (Na_2CO_3), Folin Ciocalteau reagent (FCR)]. Chemicals procured from Thomas Baker [sodium azide (NaN_3), hydrogen peroxide (H_2O_2)]. Chemicals procured from Spectrochem [1-(3-dimethylaminopropyl)-3-ethyl carbodiimide-hydrochloride (EDC·HCl), thiobarbituric acid (TBA)]. Chemicals procured from SD Fine [Epinephrine (−), Tween©80]. Chemicals procured from Hi-media [5-sulphosalicylic dihydrate acid, bovine serum albumin (BSA)]. Chemicals procured from Sigma-Aldrich [2,3,5-triphenyl tetrazolium chloride (TTC), malondialdehyde (MDA), curcumin] and Holista Colltech Limited Australia (Ovicoll Collagen).

2.2 Preparation of collagen nanoparticle

1 ml of Tween©80 was added to 40 ml of double-distilled water kept on stirring at a temperature of around 8 °C. Next, 6 mg of collagen was dissolved in 10 ml of double distilled water with continuous vortexing and sonication for proper dissolution. After 4 h, the collagen solution was added slowly to the above solution kept on stirring. Then, 3 mg EDC·HCl was added after 2 h followed by the addition of 3 mg MDA 2 h thereafter. The final reaction mixture was kept for stirring overnight. The nanoparticle aqueous solution was dialyzed for 48 h using

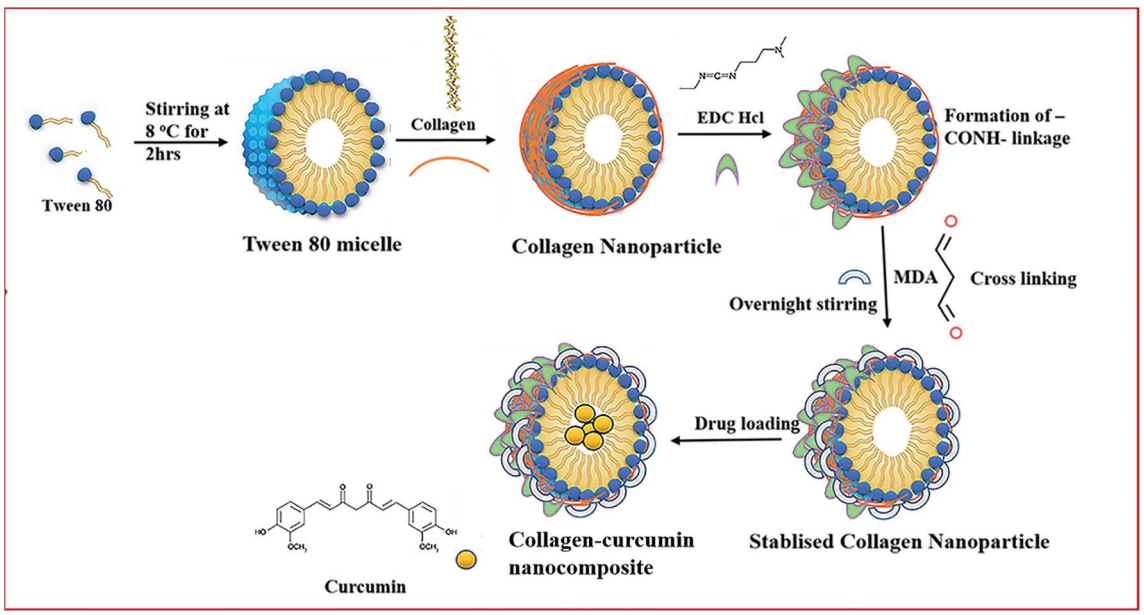

Fig. 1 Schematic representation of the preparation of collagen–curcumin nanocomposite.

spectropore membrane dialysis bag (celluSep®, 12 kD cut-off), changing the distilled water after every 4 h (Fig. 1).

2.3 Characterization of nanocomposite

2.3.1 Drug loading. A solution of curcumin in chloroform (5 mg ml^{-1}) was prepared by gentle warming with continuous vortexing. The above solution was slowly added to the aqueous solution of nanoparticle with continuous vortexing and sonication until excess drug began to settle down. Curcumin being hydrophobic goes into the core of the collagen nanoparticle. Drug loaded nanoparticle solution was then kept on dialysis for 12 h with a change of water after every 3 h for removing leftover chloroform. The dialyzed drug-loaded nanoparticle solution was then lyophilized and kept for further use.

2.3.2 Physicochemical characterization. Fourier transform infrared spectroscopy (FT-IR) was done to analyze if cross-linking has taken place in collagen nanoparticle on the addition of EDC·HCl and MDA. It was done on a Bruker alpha instrument and the spectrum was recorded in the range 4000 cm^{-1} to 400 cm^{-1}. Dynamic Light Scattering (DLS) analysis was done to determine nanoparticle size distribution and its average size determined using Zetasizer Nano ZS (Malvern Instruments Corp., Malvern, UK). Size measurement was done at 4 °C using a disposable folded capillary cell. Transmission Electron Microscopy (TEM) analysis gives nanoparticle shape and size, few drops of nanoparticles were dropped cast on a copper grid and negative staining done using 1% PTA. TEM was done at AIIMS, New Delhi on a TALOS instrument (Thermo Fischer Scientific, USA).

2.3.3 Encapsulation efficiency (EE%) calculation. It is defined as the percentage of drug that has gone inside the nanoparticles relative to the total drug added. It specifies the amount of drug that has been encapsulated into the nanoparticles and the amount of free drug still present in the dispersion medium. The encapsulation efficiency (EE%) of collagen–curcumin nanocomposite was determined by centrifuging the nanocomposite at 4 °C for 30 min at 14 000 rpm and then measuring the unentrapped (free) curcumin by taking the absorbance of the supernatant at 435 nm. EE% was calculated as follows:

$$EE\% = [(curcumin_{total} - curcumin_{free})/curcumin_{total}] \times 100$$

where $curcumin_{total}$ is the total amount of curcumin that has been loaded into the nanoparticle and $curcumin_{free}$ is the amount of free curcumin present in the solution.

The loading efficiency (LE%) reflects the amount of drug associated with a unit weight of nanoparticle. LE% can be calculated as follows:

$$LE\% = [(curcumin_{total} - curcumin_{free})/(wt\ of\ nanoparticles)] \times 100$$

2.3.4 *In vitro* release kinetics of drug from nanocomposite. The *in vitro* release kinetics study of the drug from a nanocarrier plays an important part in the development of a good nanocarrier. In this study *in vitro* release kinetics of curcumin from nanocomposite was investigated using the dialysis bag method. In this method about 100 mg of lyophilized nanocomposite powder was dissolved in 1 ml of distilled water and kept for dialysis in a beaker containing 50 ml of phosphate buffer solution (pH = 7.4, containing 1% Tween©80) for 48 h, it provides proper sink conditions as curcumin has very low aqueous solubility. In order to mimic biological conditions, the whole process was done in an incubator maintained at 37 °C. After specific time intervals about 2 ml of solution from the sink medium containing released curcumin was withdrawn, simultaneously replacing it with an equal volume of fresh phosphate buffer saline (PBS) solution. Alongside a similar setup was prepared for determining release kinetics of free curcumin dissolved in DMSO. The amount of released curcumin in the above-withdrawn sink medium was determined spectrophotometrically by taking absorbance at 435 nm and using a standard absorbance curve of curcumin in DMSO.

The percentage of curcumin released was determined as follows:

$$Release\ (\%) = \{[curcumin]_{released}/[curcumin]_{total}\} \times 100$$

where $[curcumin]_{released}$ is the concentration of curcumin released at time t, and $[curcumin]_{total}$ is the concentration of total curcumin entrapped inside the nanocomposite.

2.3.5 Storage stability of collagen nanoparticles. The size and polydispersity index (PDI) of collagen nanoparticles kept at 8 °C was monitored over a time duration of eight weeks to study their physical storage stability. The particle size and PDI were studied by taking DLS every week for eight weeks and it was found that collagen nanoparticles were physically stable during the said duration showing consistent size and peaks in DLS analysis, moreover, PDI was found to be around 0.2 with no signs of agglomeration.

2.4 *In vivo* studies

2.4.1 Animal ethics. All *in vivo* animal experiments were performed following the guidelines approved by the Committee for Control and Supervision of Experiments on Animals (CPCSEA) under the Government of India. The animals were used after taking permission and following the strict guidelines of the Institute Animal Ethics Committee (registration no. 173/GO/Re/2000/CPCSEA) of Jamia Hamdard (New Delhi, India).

2.4.2 Experimental protocol. Animal experiments were performed on female albino Wistar rats weighing between 250 g and 300 g. Rats were kept at Central Animal House Facility (CAHF), Jamia Hamdard, in polypropylene cages in air-conditioned rooms with the temperature around 25 °C and were given pellet diet and water *ad libitum* under constant dark and light cycles. For studying the neuroprotective effects of collagen–curcumin nanocomposites, the MCAO model was used. Animals were mainly divided into 6 groups each group having 6 animals ($n = 6$). The 1st group was marked as control (N) and this group animal were given void collagen nanoparticles intraperitoneally (i.p.); 2nd group was marked as ischemic (I), in this group MCAO was performed for 1 h

duration followed by reperfusion for a period of 24 h; in the 3rd group, MCAO was performed for 1 h followed by treatment with nanocomposite dose ND1 – 1 μg per kg b. wt; in the 4th group, MCAO was performed for 1 h followed by treatment with nanocomposite dose ND2–10 μg per kg b. wt; in 5th group MCAO was performed for 1 h followed by treatment with nanocomposite dose ND3–100 μg per kg b. wt and 6th group MCAO was performed for 1 h followed by treatment with free curcumin 100 μg per kg b. wt. In all the treatment groups nanocomposite was administered just after removal of occluding monofilament. After 24 h reperfusion period, a neurobehavioral assessment was done and later animals were sacrificed and brains were excised for biochemical estimations, infarct analysis, histopathology and immunohistochemistry studies.

2.4.3 Induction of transient focal cerebral ischemia by MCAO. The MCAO was performed by an intraluminal filament model.[14] Chloral hydrate (400 mg per kg b. wt) was given intraperitoneally as an anesthetic, then a polylysine coated monofilament (Doccol corporation, USA) having a smooth and flexible tip was inserted into the external carotid artery (ECA) and slowly pushed into the middle cerebral artery (MCA) *via* the internal carotid artery (ICA) for a length of 17 to 20 mm until a slight resistance was felt, the resistance indicates that the filament has crossed the proximal portion of the anterior cerebral artery (ACA). At this point, the intraluminal suture blocks the origin of MCA and obstructs every source of blood flow from the posterior cerebral artery (PCA), ACA and ICA. The intraluminal filament was slowly withdrawn 1 h after the induction of ischemia and then the animals were returned back to their cages. In the control group, ECA was exposed but no suture was inserted. The animals were later returned back to their cages and kept for 24 h reperfusion.

2.4.4 Behavioral studies. Behavioral studies included Spontaneous Motor Activity (SMA),[15] flexion test (FT)[16] and grip strength[17] test analysis using reported methods. A detailed experimental protocol for behavior studies has been provided in the ESI.†

2.4.5 Infarct analysis. In this investigation, albino Wistar rats were sacrificed and their brains were excised and kept in brain matrix (zivic instruments) after removing the hind region, 3 mm coronal sections of the brain were sliced and stained in a solution of 0.1% TTC in PBS. Succinate dehydrogenase reduces TTC into a red-colored formazan in the viable region and it remains unstained or pale in the non-viable infarct region. The quantification of infarct volume was done by measuring ischemic and non-ischemic areas using image J (Image J, Bethesda, MD) software.

2.4.6 Biochemical studies. The animals were sacrificed, and brains were dissected to take out the cortex region. The homogenization of tissue at 5% (w/v) was done in 10 mmol L^{-1} PBS (pH 7.4) and then centrifuged at 800 × *g* for 5 min at a temperature of 4 °C to get initial supernatant. A portion of the initial supernatant was taken for doing the assay of thiobarbituric acid reactive substances (TBARS), whereas the remaining portion was centrifuged at 10 500 × *g* for 15 min at 4 °C. The supernatant obtained after second-time centrifugation was used for the estimation of various antioxidant enzymes like reduced glutathione (GSH), glutathione-*S*-transferase (GST), reduced glutathione (GR), glutathione peroxidase (GP_X), superoxide dismutase (SOD), catalase (CAT) and measurement of lipid peroxidation (LPO).

Biochemical parameter estimations including measurement of LPO,[18] GSH,[19] GR,[20] GP_X,[21] SOD,[22] CAT,[23] GST[24] and protein estimation[25] were performed using reported methods. The detailed experimental protocol has been provided in the ESI.†

2.4.7 Histopathology. The rats were sacrificed and the cortex sections of the brain were embedded in paraffin. The coronal sections of thickness about 5 μm having cortex region were processed for Hematoxylin and eosin staining. The slide analysis and imaging were done using a Motic AE30 microscope.

2.4.8 Immunohistochemical study. The immunostaining was performed according to the procedure mentioned in ThermoScientific Ultra Vision ONE Large Volume Detection System HRP Polymer (Ready-To-Use) kit.[26,27] Paraffin sections were dewaxed with dimethyl benzene and graded ethanol series. After heat-induced antigen retrieval, to reduce nonspecific background staining due to endogenous peroxidase, incubated sections were processed through 4% H_2O_2 for 15 min, and then applied ultra V block and incubated for 5 min at room temperature to block nonspecific background staining. Sections were incubated with primary NF-κB (Sigma Aldrich, USA), primary COX-2 and primary caspase-3 at room temperature for 1 h. The HRP polymer (Abcam, USA) was applied to the sample and incubated for 30 min at room temperature followed by washing with TBS buffer and further incubation with DAB for 5 min. Finally, counterstaining was done using hematoxylin. The slides were then washed, dried and mounted with DPX and studied under an Olympus BX51 microscope.

2.5 Statistical analysis

The data from individual groups were presented as the mean ± standard error of the mean (S.E.M.). Differences between groups were analyzed using ordinary one-way analysis of variance (ANOVA) followed by a post hoc Tukey's multiple comparisons test using Graph Pad Prism 8 (Graph Pad Software, San Diego, CA, USA) and minimum criterion for statistical significance was set at $p < 0.05$ for all comparisons.

3. Results and discussion

3.1 Physicochemical characterization

3.1.1 FT-IR analysis. FT-IR results (Fig. 2) show that pure collagen shows a characteristic FT-IR spectrum, with the appearance of amide I peak at ~1650 cm^{-1} and amide II peak at ~1560 cm^{-1}. The amide I peak results from the stretching vibration of the peptide carbonyl group (–CO) and amide II results from –NH bending vibrations. In FT-IR of collagen nanoparticles –NH bending peak has disappeared showing the formation of additional amide (–CONH) bonds after the addition of carboxyl-amine coupling reagent EDC·HCl and peak of carbonyl group (–CO) stretching is retained. Moreover, the

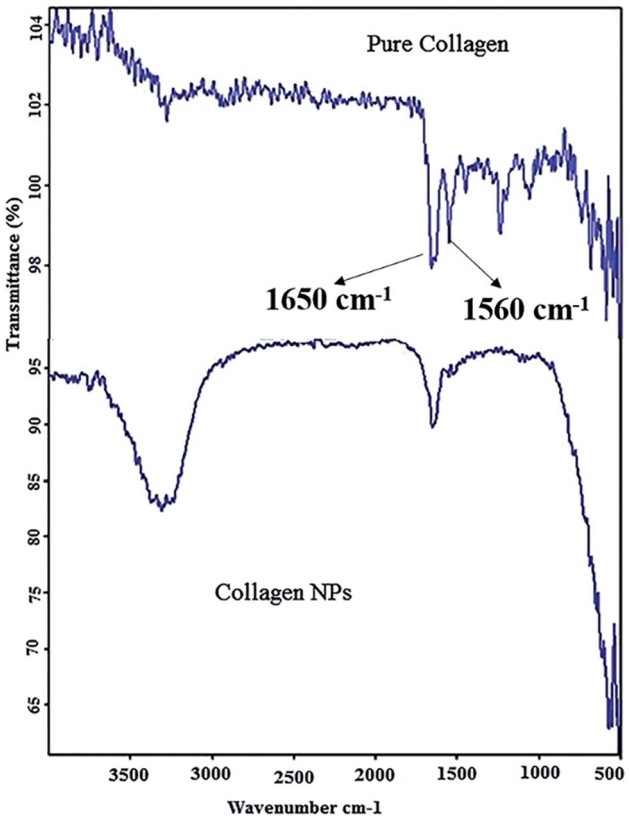

Fig. 2 Fourier Transform Infrared (FT-IR) spectra of pure collagen (top) and collagen nanoparticles (below).

intensity of peaks between 1000 cm^{-1} and 1500 cm^{-1} has decreased considerably showing extensive amide bond formation after adding EDC·HCl and cross-linker malondialdehyde (MDA) resulting in stabilization of collagen nanoparticles.

3.1.2 DLS and HR-TEM analysis. The size analysis of the nanoparticles was done using DLS and TEM techniques. DLS showed collagen–curcumin nanocomposite has an average hydrodynamic diameter of around 120 nm (Fig. 3A) and a polydispersity (PDI) of 0.266. The nanocomposite showed a size of around 65 nm and a spherical morphology in TEM (Fig. 3B).

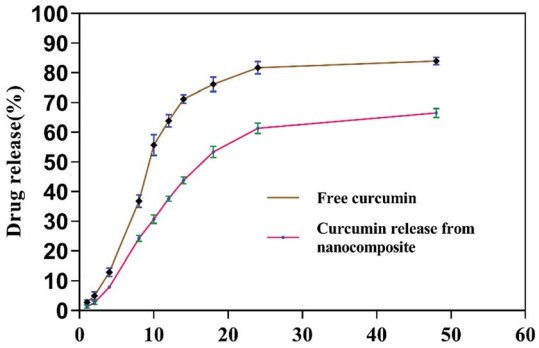

Fig. 4 The *in vitro* release kinetics profile of curcumin from nanocomposite.

3.1.3 Entrapment efficiency and *in vitro* release kinetics study. The collagen–curcumin nanocomposite encapsulation efficiency EE% was found to be about 80% with a loading efficiency of 2%. There lease kinetics showed as low and sustained release of curcumin from nanocomposite in phosphate buffer at the physiological pH = 7.4 as compared to the release of free curcumin under similar conditions (Fig. 4).

3.2 *In vivo* studies results

The animal studies were conducted on albino Wistar rats. After induction of focal cerebral ischemia using MCAO model, animals were treated with collagen–curcumin nanocomposite doses of ND1 (1 μg per kg b. wt), ND2 (10 μg per kg b. wt), ND3 (100 μg per kg b. wt) and free curcumin (FD) dose of (100 μg per kg b. wt). After a reperfusion period of 24 h animals were assessed for behavioral studies and later sacrificed for studying various *in vivo* parameters.

3.2.1 Behavioral parameters analysis. Cerebral ischemia/reperfusion injury caused significant impairment in motor

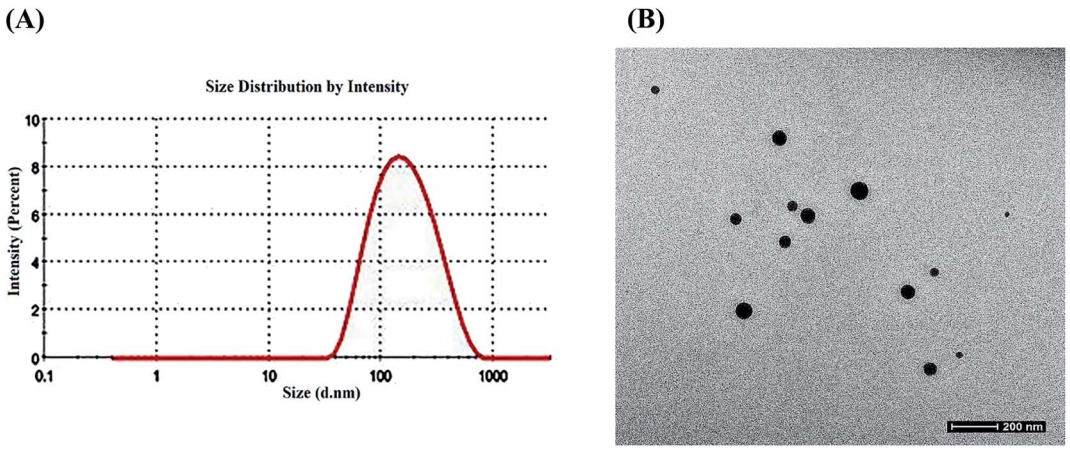

Fig. 3 (A) Dynamic light scattering pattern of the collagen–curcumin nanocomposite. (B) Transmission electron microscopy of the collagen–curcumin nanocomposite.

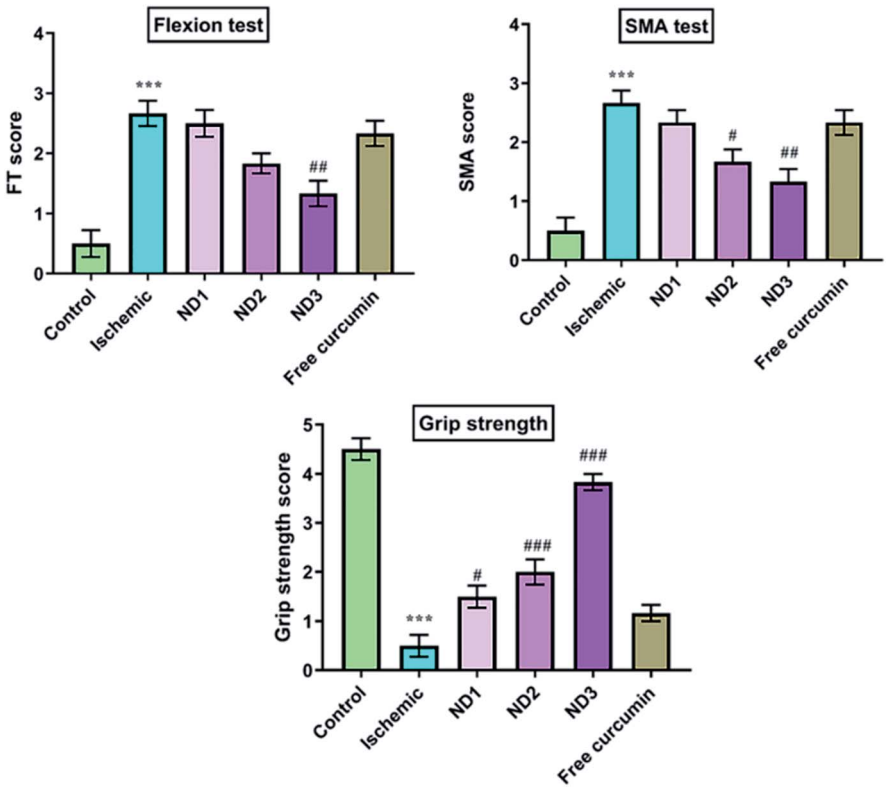

Fig. 5 Effect of collagen–curcumin nanocomposite on behavioral parameters like FT, SMA and grip strength for control (N), ischemic (I), ND1 (1 μg per kg b. wt), ND2 (10 μg per kg b. wt), ND3 (100 μg per kg b. wt) and free curcumin (FD) (100 μg per kg b. wt). The motor deficit was significant in the ischemic (I) group in comparison to the control (N) group. Treating the animals with nanocomposite has decreased motor deficit and improved grip strength significantly, especially at ND3 dose. Values are expressed as mean ± S.E.M. Results on comparison with the control group shows a significant difference (***$p < 0.001$). Results obtained shows significant difference from ischemic group ($^{\#}p < 0.05$, $^{\#\#\#}p < 0.001$).

performance, this could be because of neuronal damage. This results in the death of neurons in the territory of the brain being supplied blood by the MCA *i.e.* the caudate nucleus, the putamen and the striatum areas that regulate motor coordination. In this study rats were evaluated for various behavioral parameters like SMA, flexion test and grip strength and these parameters were found to show severe deficits in cerebral ischemia induction by MCAO model.[14] Treatment with

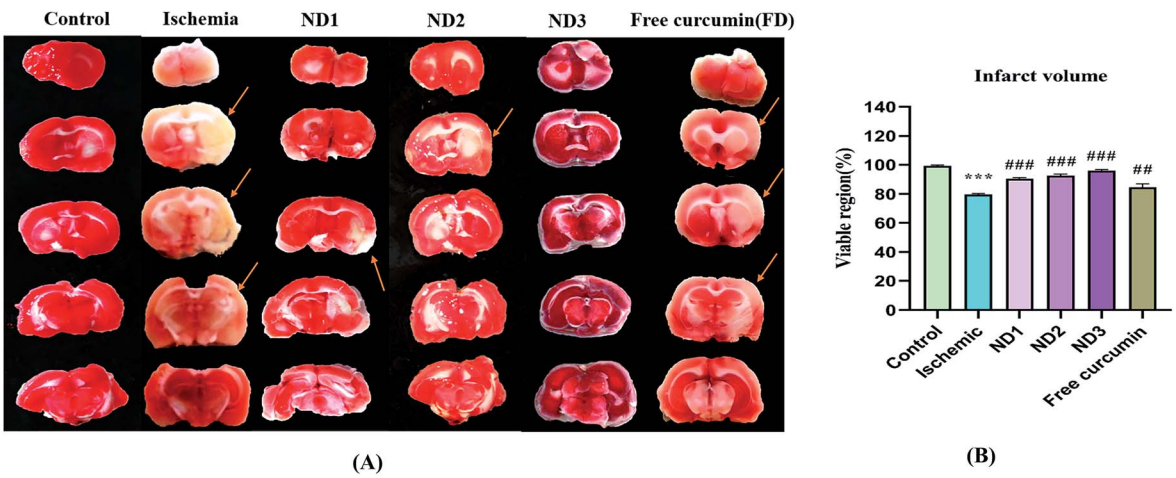

Fig. 6 (A) Photographs showing effect of collagen–curcumin nanocomposite on brain infarct in control (N), ischemic (I), ND1 (1 μg per kg b. wt), ND2 (10 μg per kg b. wt), ND3 (100 μg per kg b. wt) and free curcumin (FD) (100 μg per kg b. wt) resp. Infarct region is very well visible in ischemic group (I) brain sections as compared to control (N) group brain sections and all the three treatment groups showed a significant reduction in infarct region in comparison to free curcumin group. (B) Shows quantification of infarct analysis. Values are expressed as mean ± S.E.M. Results on comparison with the control group shows a significant difference (***$p < 0.001$). Results obtained shows significant difference from ischemic group ($^{\#}p < 0.05$, $^{\#\#\#}p < 0.001$).

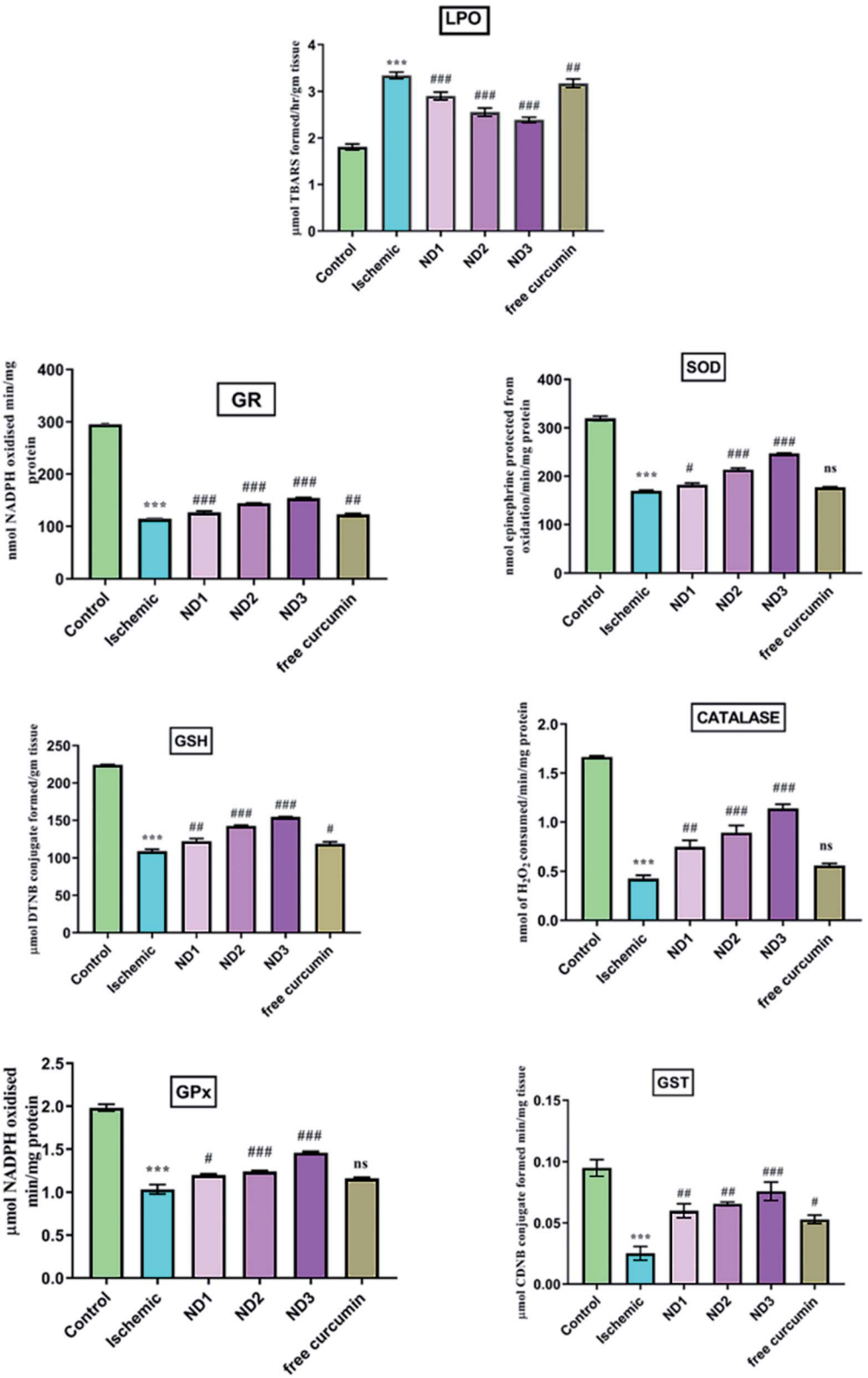

Fig. 7 Effect of collagen–curcumin nanocomposite on various biochemical markers like LPO, SOD, GSH, GP_X, GST, CATGR. Groups shown are control (N), ischemic (I), ND1 (1 µg per kg b. wt), ND2 (10 µg per kg b. wt), ND3 (100 µg per kg b. wt) and free curcumin (FD) (100 µg per kg b. wt). A significant increase in LPO content and decrease in other anti-oxidant marker content can be seen in ischemic (I) group in comparison to control (N) group. Treatment with ND3 restored the marker content significantly. Results are shown as mean ± S.E.M. Results on comparison with control group shows significant difference (***$p < 0.001$). Results obtained shows significant difference from ischemic group ($^{\#}p < 0.05$, $^{\#\#}p < 0.01$, $^{\#\#\#}p < 0.001$ and ns $p > 0.05$).

nanocomposite restored neurological deficit to a significant level as is evident in results (Fig. 5) with ND3 dose showing best results, even ND1 dose shows better results than free curcumin dose. The poor neurobehavioral score in ischemic rats could be due to generation of free radicals that result in loss of motor coordination and locomotion in the caudate–putamen and sensorimotor cortices as a result of necrosis induction in these regions.[28]

3.2.2 Analysis of infarct volume. The extent of injury to brain regions (cortex, striatum, and hippocampus) after induction of cerebral ischemia by MCAO depends on the time of occlusion of the MCA and reperfusion period.[29,30] Infarct analysis by TTC staining clearly depicts the extent of infarction in the brain. TTC acts like a proton acceptor for many pyridine nucleotide linked dehydrogenases (especially succinate dehydrogenases) along with the cytochromes that form an integral part of inner mitochondrial membrane and make up the electron transport chain, tetrazolium salt which is white in color is reduced by enzymes into a red lipid-soluble formazan in the viable tissues and the infarct region remains unstained, this is due to loss of enzyme activity in affected regions when mitochondria are put to stress, as a result of reduction in blood supply to the brain. In the study using TTC infarct analysis, infarction is very well visible in the striatum, cortex and the hippocampus regions in the ischemic (I) group which has reduced considerably in the treatment groups ND1, ND2, ND3, and free curcumin, best results given by ND3 over other three treatments, in comparison to ischemic (I) group (Fig. 6A). Results have been quantified by plotting percentage viable region for all the animal groups (Fig. 6B).

3.2.3 Biochemical parameter analysis. Cerebral ischemia/reperfusion injury leads to the generation of free radicals in excess upon blood reflow and failure of tissue antioxidant activity results in oxidative stress-induced neuronal loss. During

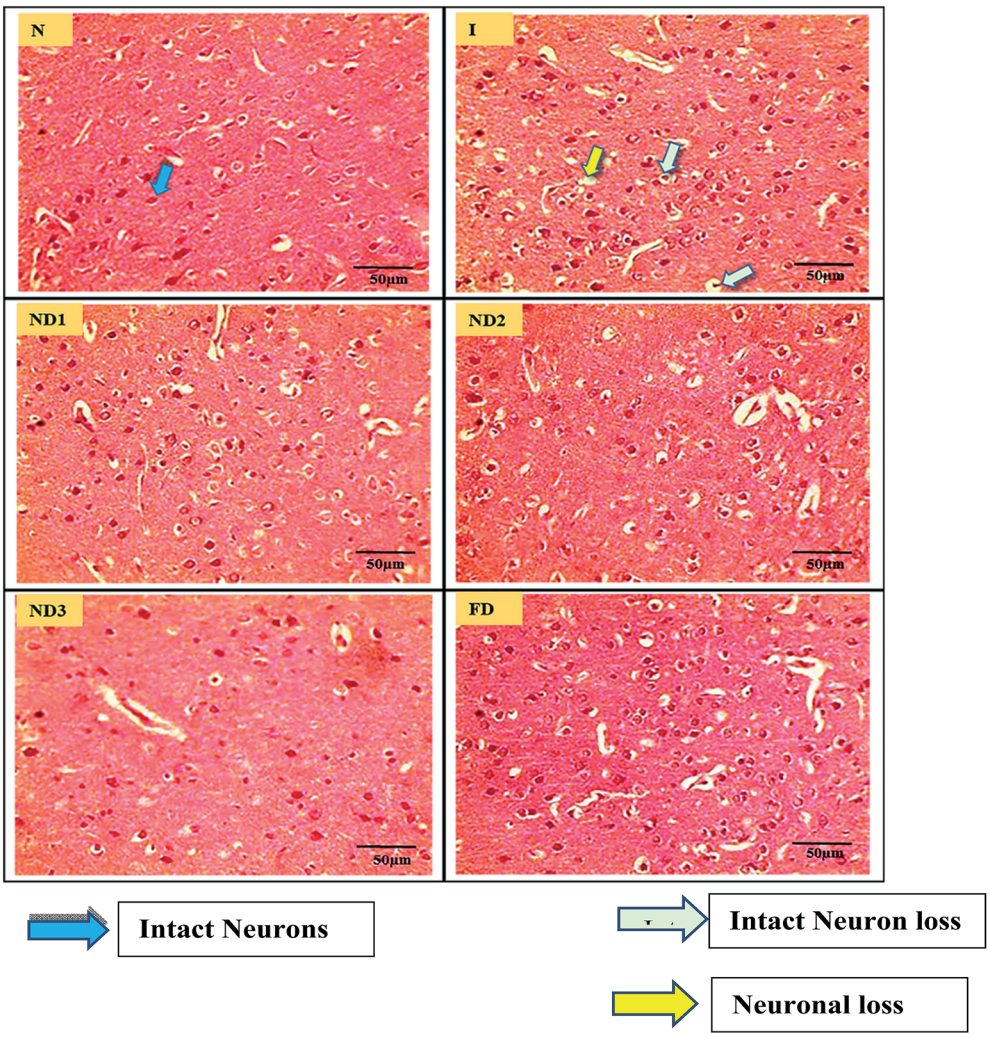

Fig. 8 Photographs (magnification = 40×, scale = 50 μm) showing histopathological changes in the cortex region for all the groups *i.e.* control (N), ischemic (I), collagen–curcumin nanocomposite doses of ND1 (1 μg per kg b. wt), ND2 (10 μg per kg b. wt), ND3 (100 μg per kg b. wt) and free curcumin (FD) (100 μg kg^{-1} b. wt). Control (N) group shows intact neurons and morphology, whereas in ischemic (I) group degenerative changes like neuronal loss, vacuolation (loss of intact neurons) and altered morphology are clearly visible. ND1 treatment group shows decreased vacuolation and less morphological changes, these results are further improved in ND2 and ND3 when compared with ischemic (I) and free curcumin treatment groups.

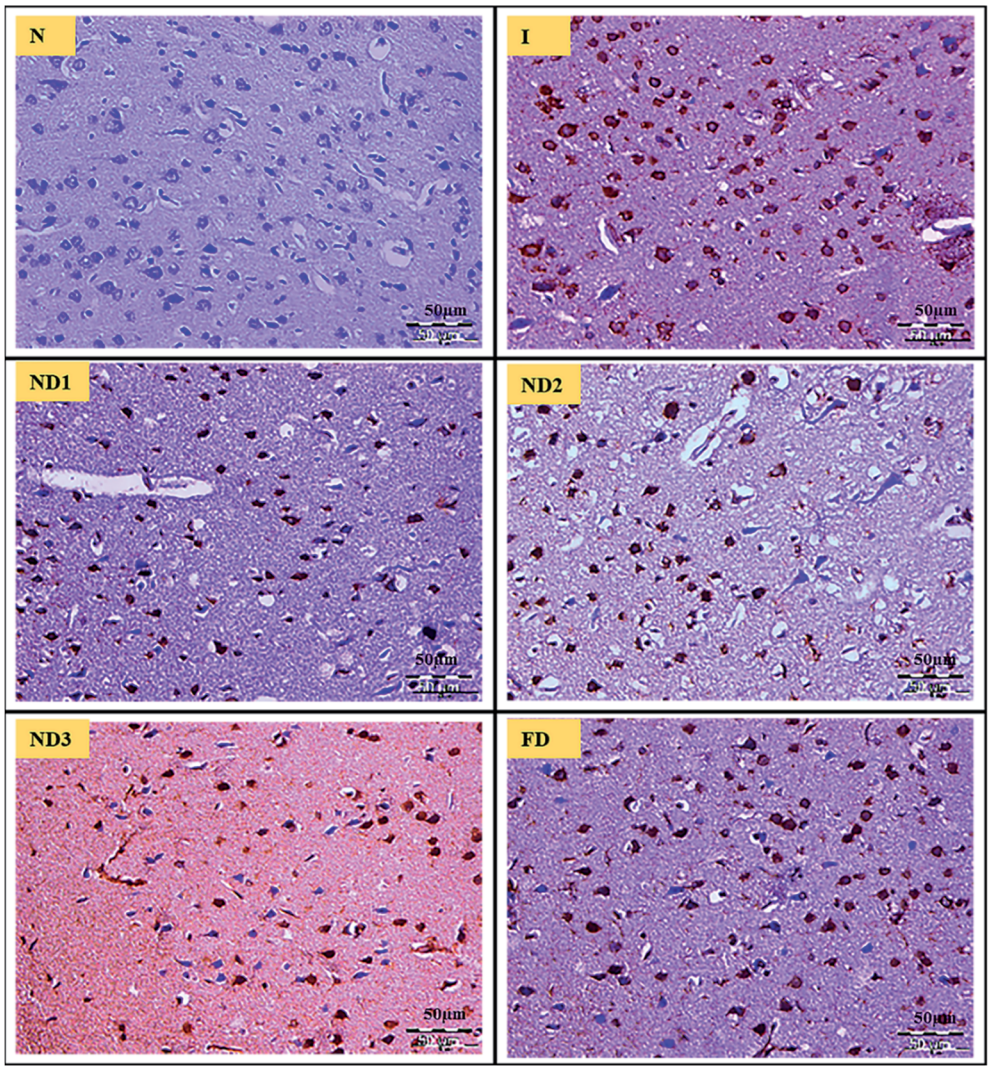

Fig. 9 Photographs (magnification = 40×, scale = 50 μm) shows immunohistochemical expression of NF-κB in MCAO model in control (N), ischemic (I) and treatment groups of collagen–curcumin nanocomposite doses ND1 (1 μg per kg b. wt), ND2 (10 μg per kg b. wt), ND3 (100 μg per kg b. wt) and free curcumin (FD) (100 μg per kg b. wt). Control (N) group shows no expression for the NF-κB marker whereas the ischemic (I) group shows maximum expression. Treatments ND1 and ND2 show moderate expression but less than free curcumin, ND3 shows minimum expression.

reperfusion there is an abrupt supply of molecular oxygen which acts as a substrate for xanthine oxidase for nucleotide metabolism, this leads to an increase in the generation of H_2O_2 and superoxide as by-products.[31] This explosive production of free radicals combined with peroxides and superoxides increases damage to the tissue. TBARS content is indicative of LPO and is a measure of oxidative stress. A high content of LPO in form of TBARS in ischemic group found as has been reported earlier,[32] the GSH content is lowered in ischemic group due to it being consumed in scavenging rapidly generated reactive oxygen species (ROS),[33] leading to reduction in content of GSH dependent enzymes like (GP_X, CAT, GR, GST) and SOD that too act as ROS scavengers.[34] The results showed a decrease in GSH content in the ischemic group and enzymes dependent on it like SOD, CAT, GP_X, GR and GST in comparison to the control group (Fig. 7). Treatment with nanocomposite increases the GSH content in comparison to the ischemic (I) group significantly and enzymes dependent on it showed similar results especially ND3 dose (Fig. 7). Curcumin has been known to increase reduced glutathione under oxidative stress.[35] Curcumin interacts with oxidative cascade by neutralizing or scavenging of free radicals and inhibiting LPO.[36] Curcumin possesses both phenolic and β-diketone functional groups and that makes it a potent antioxidant and free radical scavenger.[37] In addition, curcumin is known to enhance the activities of antioxidant enzymes such as SOD, CAT and GP_x.[38] In mitochondria, the curcumin reduces ROS and prevents oxidative damage.[39]

3.2.4 Histopathological analysis. MCAO induction leading to ischemia/reperfusion injury triggers generation of ROS species leading to a state called oxidative stress that comprises of a cascade of events resulting in decrease in level of antioxidant enzymes like glutathione, increase in LPO levels and

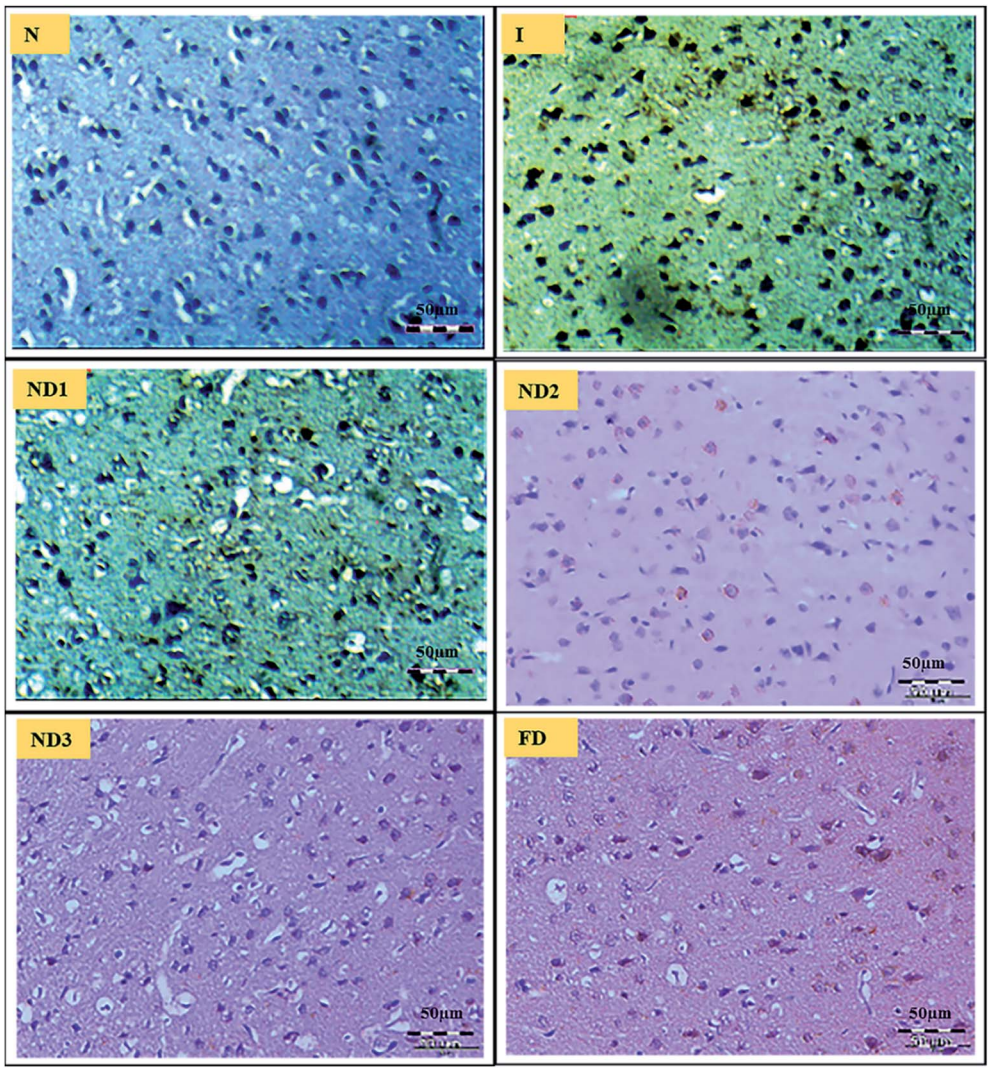

Fig. 10 Photograph (magnification = 40×, 5 μm) shows immunohistochemical expression of COX-2 in MCAO model in control (N), ischemic (I) and treatment groups of nanocomposite doses ND1 (1 μg per kg b. wt), ND2 (10 μg per kg b. wt), ND3 (100 μg per kg b. wt) and free curcumin (FD) (100 μg per kg b. wt). Control (N) group shows almost no expression for the COX-2 marker whereas the ischemic (I) group shows maximum expression. Treatments ND1 and ND2 show moderate to mild expression but less than free curcumin, ND3 shows almost no expression.

disturbances in redox state of the cells due to ionic imbalances.[40] All these factors lead to neurodegenerative losses which are very well reflected in brain histopathological results. The sections of the control (N) group showed normal neuronal cells without any pathological changes, whereas sections of the ischemic (I) group showed brain damage accompanied by neuronal loss, lack of intact neurons and presence of many vacuolated spaces (Fig. 8). Treatment with collagen–curcumin nanocomposite doses ND1 and ND2 showed better results than free curcumin showing partial neuronal loss with the presence of intact neurons in between vacuolated spaces whereas treatment ND3 showed best results restoring histopathology almost near to the control (N) group (Fig. 8).

3.2.5 Immunohistopathological analysis. Ischemic stroke induction by the MCAO model resulted in inflammation due to the release of inflammatory molecules like NF-κB and COX-2 that are responsible for cell death.

Inflammatory marker NF-κB is known to be activated by a variety of stimuli that occur in focal cerebral ischemia, such as glutamate,[41] hypoxia, and ROS.[42] It is a transcriptional activator of a number of genes involved in the pathogenesis of cerebral ischemia for *e.g.* iNOS and COX-2, also NF-κB expression increases with increase in ROS generation.[43] Curcumin is known to suppress activation of nuclear factor NF-κB,[44] which is very well demonstrated in the results as ischemic (I) group shows increased expression of NF-κB in comparison to control (N) group, treatment with nanocomposite reduced the expression significantly in ND3 (Fig. 9).

Curcumin shows inhibitory activity over COX-2.[45] Curcumin shows an inhibitory effect on neuroinflammatory response to cerebral ischemia of rat through activating the PPARγ pathway. There are numerous pieces of evidence clearly showing that activation of PPARγ confers to neuroprotective effect in the experimental models of ischemic injury,[46] curcumin might be a likely agonist of PPARγ which is known to suppress COX-2

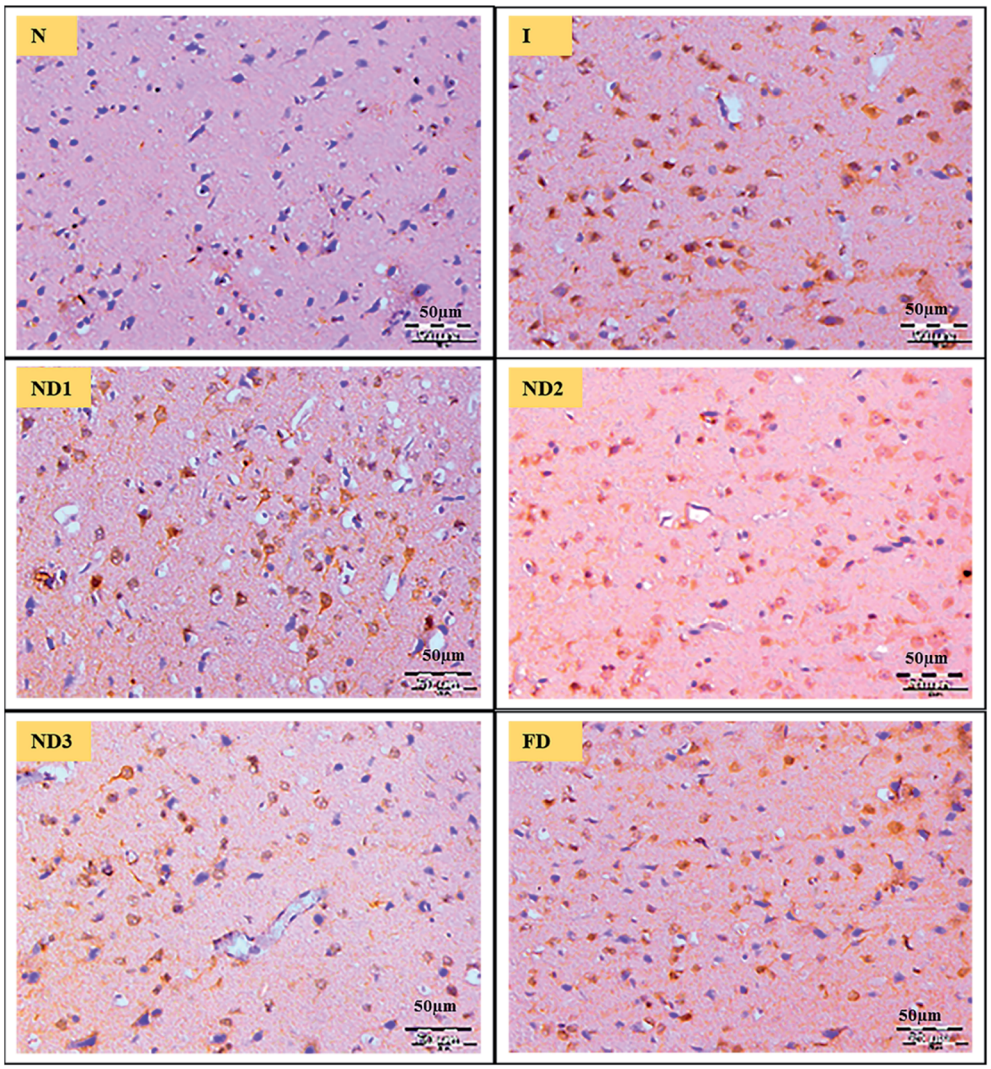

Fig. 11 Photograph (magnification = 40×, scale = 50 μm) shows immunohistochemical expression of caspase-3 in MCAO model in control (N), ischemic (I) and treatment groups of nanocomposite doses ND1 (1 μg per kg b. wt), ND2 (10 μg per kg b. wt), ND3 (100 μg per kg b. wt) and free curcumin (FD) (100 μg per kg b. wt). Control (N) group shows almost no expression for caspase-3 marker whereas the ischemic (I) group shows maximum expression. Treatments ND1 and ND2 show moderate to mild expression but less than, ND3 shows minimum expression.

expression in cerebral ischemia of rats. Further verifying the data the results showed that the expression of COX-2 increased in cerebral ischemic rats. Treatment with nanocomposite significantly decreased COX-2 expression, best results are shown by nanocomposite dose of ND3 followed by ND2 and ND1 in comparison to free curcumin dose (Fig. 10), these results clearly present the beneficial effects of curcumin against cerebral ischemic injury due to suppression of inflammatory response by activating PPARγ.

Mitochondrial impairment and oxidative stress lead to damage to neurons and ends up inactivation of an apoptotic stage. It is already known that cerebral ischemia induces the activation of caspase-3, neuronal death is preceded by the up-regulation and activation of caspase-3. Curcumin could reduce the loss of the neurons in ischemic brain tissue, and it inhibits expression of the activated caspase-3, an important executor of apoptosis.[47] There is a substantial neuronal death after transient focal cerebral ischemia, initiated by caspase-3 activity and it contributes to the delayed loss of neurons from the penumbral region of infarct area.[48–50] In this study, neuronal loss was observed in the cortex region after transient focal cerebral ischemia. After the administration of nanocomposite, the expression of activated caspase-3 was apparently inhibited in treatment group ND3 more prominently as compared to the ischemic (I) group (Fig. 11), treatments ND1 and ND2 showed better results than free curcumin.

4. Conclusions

The findings of this study clearly suggest that the neuroprotective effect of curcumin on cerebral ischemic damage in MCAO reperfusion rats have been significantly enhanced by using collagen–curcumin nanocomposite. The major success achieved using nanocomposite could be very well defined by

increased bioavailability and improved permeability across the BBB, which has helped in producing far more effective results in comparison to free curcumin and that too at very low concentrations. These findings by improving upon the already known neuroprotective potential of curcumin could pave the way for a future research avenue for exploring numerous benefits for other neurodegenerative diseases.

Conflicts of interest

There are no conflicts to declare.

Abbreviations

MCAO	Middle cerebral artery occlusion
COX-2	Cyclooxygenase-2
BBB	Blood–brain barrier
NF-κB	Nuclear factor kappa-light-chain-enhancer of activated B cells
DMSO	Dimethyl sulfoxide
HRP	Horseradish peroxidase
PPARγ	Peroxisome proliferator-activated receptor gamma

Acknowledgements

The authors are extremely thankful to Jamia Hamdard for providing the prestigious Silver Jubilee Fellowship that was of great help in carrying out this research. Also, the authors would like to thank Dr Ambrish Kumar Tiwari, Incharge CAHF, Jamia Hamdard for his help in all histopathological and immunohistochemical interpretations.

References

1 X. Q. Liu, R. Sheng and Z. H. Qin, *Acta Pharmacol. Sin.*, 2009, **30**, 1071–1080.
2 U. Dirnagl, C. Iadecola and M. A. Moskowitz, *Trends Neurosci.*, 1999, **22**, 391–397.
3 E. Z. Longa, P. R. Weinstein, S. Carlson and R. Cummins, *Stroke*, 1989, **20**, 84–91.
4 J. L. Cheatwood, A. J. Emerick, M. E. Schwab and G. L. Kartje, *Stroke*, 2008, **39**, 2091–2098.
5 J. Castillo, R. Rama and A. Davalos, *Stroke*, 2000, **31**, 852–857.
6 P. Chabrier, M. Auguet, B. Spinnewyn, S. Auvin, S. Cornet, C. Demerle-Pallardy, *et al.*, *Proc. Natl. Acad. Sci.*, 1999, **96**, 10824–10829.
7 Y. Wang, C. F. Chang, H. L. Chen, X. Deng, B. K. Harvey and J. L. Cadet, *Exp. Neurol.*, 2005, **193**, 75–84.
8 W. M. Pardridge, *Drug Discovery Today*, 2007, **12**, 54–61.
9 R. C. Srimal and B. N. Dhawan, *J. Pharm. Pharmacol.*, 1973, **25**, 447–452.
10 F. Yang, G. P. Lim, A. N. Begum, O. J. Ubeda, M. R. Simmons, S. S. Ambegaokar, *et al.*, *J. Biol. Chem.*, 2005, **280**, 5892–5901.
11 C. Yang, X. Zhang, H. Fan and Y. Liu, *Brain Res.*, 2009, **1282**, 133–141.
12 T. Miyata, T. Taira and Y. Noishiki, *Clin. Mater.*, 1992, **9**, 139–148.
13 W. Sun, C. Xie, H. Wang and Y. Hu, *Biomaterials*, 2004, **25**, 3065–3071.
14 E. Z. Longa, P. R. Weinstein and S. Carlson, *Stroke*, 1989, **20**, 84–91.
15 S. S. Raza, M. M. Khan, M. Ashafaq, A. Ahmad, G. Khuwaja, A. Khan, *et al.*, *J. Neurol. Sci.*, 2011, **309**, 45–54.
16 Vaibhav, P. Shrivastava, H. Javed, A. Khan, M. E. Ahmed, R. Tabassum, *et al.*, *Mol. Cell. Biochem.*, 2012, **367**, 73–84.
17 P. M. Moran, L. S. Higgins, B. Cordell and P. C. Moser, *Proc. Natl. Acad. Sci. U. S. A.*, 1995, **92**, 5341–5345.
18 H. C. Utley, F. Bernheim and P. Hochslein, *Arch. Biochem. Biophys.*, 1967, **260**, 521–531.
19 D. J. Jollow, J. R. Mitchell, N. Zampaglione and J. R. Gillette, *Pharmacology*, 1974, **11**, 151–169.
20 I. Carlberg and B. Mannervik, *J. Biol. Chem.*, 1975, **250**, 5475–5480.
21 J. Mohandas, J. J. Marshal, G. G. Duggin, J. S. Horvath and D. J. Tiller, *Biochem. Pharmacol.*, 1984, **33**, 1801–1807.
22 M. J. Stevens, I. Obrosova, X. Cao, H. C. Van and D. A. Greene, *Diabetes*, 2000, **49**, 1006–1015.
23 A. Claiborne, Catalase Activity, in *Handbook of Methods for Oxygen Radical Research*, ed. R. A. Greenwald, CRC Press, Boca Raton, FL1985, 1985, pp. 283–284.
24 W. H. Habig, M. J. Pabst and W. B. Jakoby, *J. Biol. Chem.*, 1974, **249**, 7130–7139.
25 O. H. Lowry, N. J. Rosebrough and A. L. Farr, *J. Biol. Chem.*, 1951, **193**, 265–275.
26 R. S. Shan, G. James, J. C. Richard, Y. Lillian, H. Debra, S. Yan, *et al.*, *Appl. Immunohistochem. Mol. Morphol.*, 1999, **7**, 201–208.
27 P. Karen, T. Rosalba and J. Daisy, *J. Histotechnol.*, 2002, **25**, 247–250.
28 A. J. Hunter, K. B. Mackay and D. C. Rogers, *Trends Pharmacol. Sci.*, 1998, **19**, 59–66.
29 E. Z. Longa, P. R. Weinstein, S. Carlson and R. Cummins, *Stroke*, 1989, **20**, 84–91.
30 C. Heurteaux, C. Laigle, N. Blondeau, G. Jarretou and M. Lazdunski, *Neuroscience*, 2005, **137**, 241–251.
31 L. D. Kong, Y. Zhang, X. Pan, R. X. Tan and C. H. Cheng, *Cell. Mol. Life Sci.*, 2000, **57**, 500–505.
32 K. S. Zafar, A. Siddiqui, I. Sayeed, M. Ahmad, S. Salim and F. Islam, *Neurochem*, 2003, **84**, 438–446.
33 Z. Liu, P. Li, D. Zhao, H. Tang and J. Guo, *Behav. Brain Funct.*, 2010, **6**, 61–66.
34 Z. Lin, D. Zhu, Y. Yan, B. Yu, Q. Wang, P. Shen and K. Ruan, *Altern. Med.*, 2011, 1–7.
35 D. Jat, P. Parihar, S. C. Kothari and M. S. Parihar, *Cell. Mol. Biol.*, 2013, **59**, 1899–1905.
36 M. Balasubramanyam, A. A. Koteswari, R. S. Kumar, S. F. Monickaraj, J. U. Maheswari and V. Mohan, *J. Biosci.*, 2003, **28**, 715–721.
37 A. C. Reddy and B. R. Lokesh, *Mol. Cell. Biochem.*, 1994, **137**, 1–8.
38 A. C. Reddy and B. R. Lokesh, *Food Chem. Toxicol.*, 1994, **32**, 279–283.

39 Y. G. Zhu, X. C. Chen, Z. Z. Chen, Y. Q. Zeng, G. B. Shi, Y. H. Su, *et al.*, *Acta Pharmacol. Sin.*, 2004, **25**, 1606–1612.
40 D. N. Granger and P. R. Kvietys, *Redox Biol.*, 2015, 524–551.
41 C. Kaltschmidt, B. Kaltschmidt and P. A. Baeuerle, *Proc. Natl. Acad. Sci. U. S. A.*, 1995, **92**, 9618–9622.
42 P. Baeuerle and T. Henkel, *Annu. Rev. Immunol.*, 1994, **12**, 141–179.
43 A. Martin-Villalba, I. Herr, I. Jeremias, M. Hahne, R. Brandt, J. Vogel, *et al.*, *J. Neurosci.*, 1999, **19**, 3809–3817.
44 S. Singh and B. B. Aggarwal, *J. Biol. Chem.*, 1995, **270**, 24995–25000.
45 C. V. Rao, T. Kawamori, R. Hamid and B. S. Reddy, *Carcinogenesis*, 1999, **20**, 641–644.
46 W. Gillespie, N. Tyagi and S. C. Tyagi, *Indian J. Biochem. Biophys.*, 2011, **48**, 73–81.
47 P. C. Ashe and M. D. Berry, *Biol. Psychiatry*, 2003, **27**, 199–214.
48 S. H. Graham and J. Chen, *J. Cereb. Blood Flow Metab.*, 2001, **21**, 99–109.
49 S. Love, *Biol. Psychiatry*, 2003, **27**, 267–282.
50 L. Wei, N. C. Suwanwela and P. Suthiluk, *Mol. Med. Rep.*, 2017, **16**, 4710–4720.